SCIENTIFIC REPORT

ACTION: ES1303 TOPROF
STSM: COST-STSM-ECOST-STSM-ES1303-030416-073304
TOPIC: Characterising Leosphere Doppler lidar performance
VENUE: Icelandic Meteorological Office (Veðurstofa Íslands), Iceland
PERIOD: 03 – 08 April 2016

Host: Guðrún Nína Petersen (Icelandic Meteorological Office, Iceland)
Applicant: Ewan O'Connor (Finnish Meteorological Institute, Finland)
Submission date: 6 May 2016

Contribution by: Guðrún Nína Petersen (Icelandic Meteorological Office, Iceland), Jana Preissler (NUIG, Ireland), Ludovic Thobois (Leosphere, France)

COST is supported by the EU Framework Programme Horizon 2020

Introduction

This STSM took place at the Icelandic Meteorological Office (IMO) in Reykjavík, Iceland, from 4-8th April, and was hosted by Guðrún Nína Petersen (IMO). Also present were Jana Preissler (NUIG, Ireland) and Ludovic Thobois (Leosphere, France).

Motivation and objectives

This STSM is dedicated to characterising the performance of Leosphere scanning windcube Doppler lidar systems. Understanding the system performance and uncertainties in the basic measurements of radial Doppler velocity and signal-to-noise ratio is vital for providing reliable products. Correct uncertainty assessment of the raw measurements is required to enable faithful propagation of uncertainties through to the higher-level products that are created, such as wind speed and direction, turbulent properties, and attenuated backscatter.

The role of the Doppler lidar working group in TOPROF is to ensure a coherent set of Standard Operating Procedures and a data processing framework is available for operators of all viable Doppler lidar systems that might be utilised within an emerging European Doppler lidar network with the goal of providing harmonised retrievals. This requires a thorough evaluation of the measurement setup, scan selection and processing chain of each system to enable them to become members of a network capable of providing reliable winds and turbulent parameters in the boundary-layer.

This STSM concentrated on the Leosphere WindCube 200S, a full-hemispheric scanning Doppler lidar system which is available with and without depolarisation capability. There are currently 3 of these systems within the nascent European meteorological Doppler lidar network, located at:

- Mace Head (Ireland)
- Keflavík (Iceland)
- Reykjavík (Iceland) – mobile system

The mobile system at Reykjavík is mounted within a trailer for emergency deployment anywhere in Iceland.

The specific tasks for this STSM covered:

- Outline of current operating procedures, scan selection and instrument performance
- Describe current processing chains for Leosphere instruments
- Highlight actual and potential instrument issues
- Perform specific scans and evaluate results
- Characterise performance:
    - velocity uncertainty
    - signal uncertainty
    - background correction
    - telescope focus function
- Identify additional processing steps required
- Begin definition of tests and processing tools necessary to harmonise Leosphere Doppler lidar data
- Optimise scan strategy
- Update current processing chains where necessary
- Begin writing Standard Operating Procedures document for Leosphere systems

Current operating procedures and processing

Jana Preissler outlined the current operating procedures at Mace Head, and introduced her processing routines which will form the core of a common Leosphere processing chain within the network. The processing routines obtain unfiltered raw data, including the spectra, from the instrument via mysql commands. This is then processed to netcdf. The language used is **Python**.

The original processing scheme was monolithic, in that it performed all processing steps at once, and provided all scans for the day within a single file. A decision was taken to move towards a more modular approach for the processing framework. This would not only allow flexibility into the processing, it would allow a more fine-grained control over the intermediate processing steps, output different scan types in different files, and aid debugging. An additional major benefit is that this would allow the integration of other pre-written routines for specific variables, uncertainties or products, and place the processing framework for the Leosphere instruments within a common Doppler lidar processing framework for the entire network. This ensures harmonised processing across the network and would also reduce the workload for each individual operator.

To enable this, the Leosphere processing code is being checked to ensure the consistency of variable naming and attributes within the processed netcdf files, and updated to include within these files specific instrument configuration parameters (e.g. PRF, pulse length, receiver bandwidth, pulse length) that are required for uncertainty quantification and higher-level products.

Documentation for the full processing framework will be provided, showing file contents at each stage.

Instrument issues

There was comprehensive discussion on some of the instrument issues encountered so far during operation, together with plans for their mitigation. See Jana Preissler's report for more discussion. In summary, it was noted that there were occasional issues with the background noise which were traced to a problem with the noise spectra (see Fig. 2). It was suggested that occasional water condensation internally or on the outside of the lens could be responsible for these bad noise spectra. The noise spectra can be used to flag the rays affected.

The background noise CNR was usually constant with range, except for the issue noted above. However, the background noise CNR was seen to change slightly from ray to ray. This could potentially be corrected for by using the technique of Manninen et al (2016), but only if the noise floor actually should be constant from ray to ray (i.e. there are the same number of pulses and pulse energy in each ray).

For one instrument in Iceland, the CNR out-of-range value is ill-chosen as it falls within the expected range for good measurements. It is constant and can be isolated but potentially removes some 'real' data. This will be checked and fixed by Leosphere.

Optimise scan strategy

The standard Leosphere VAD mode does not change the integration time per ray in a scan, it changes how many rays per scan (azimuthal resolution).

To control the accumulation time of each individual ray requires the creation of composite scans, where each LOS ray is defined separately and then combined. For example, we defined a new VAD scan from a set of 12 independent LOS rays with specified azimuth, elevation and an integration time of 5 seconds per ray. This was then compared with a standard Leosphere-defined VAD with the same number of rays that took 1/5 of the time. The noise floor was reduced by the expected amount of 5 dB which would allow a reduction in the SNR threshold, providing more data with improved velocity uncertainty. Although it does not seem intuitive that a lower velocity uncertainty

is achievable from a lower SNR value, this is because the velocity uncertainty is based on both SNR and integration time and is essentially due to better sampling statistics of both noise and signal.

A scan schedule with two VADs at different elevations was implemented; one at 75 degrees elevation from horizontal and one at 15 degrees elevation. These can be used to create vertical profiles of horizontal wind which can be merged; the low elevation scan providing high vertical resolution near the surface and filling in the blind zone from the 75 degree elevation VAD (first usable range gate is typically at 150 m).

Outcome: **Recommend core scans, define a suitable length of vertical stare, and leave space for additional optional scans.**

Additional scans were also tested and implemented within the operational scan schedule: calibration scans for both pointing direction, and for the telescope focus correction.

Velocity and signal uncertainties

The term wideband signal-to-noise ratio, SNR, refers to the ratio of the average total signal power to the average noise power over the full bandwidth. This can also be defined as the carrier-to-noise ratio, CNR.

The velocity and signal uncertainties for spectral accumulation in a heterodyne Doppler lidar are a function of wideband SNR, and can be calculated using the appropriate formulae (Pearson et al., 2009; O'Connor et al., 2010). These formulae utilise the Cramer-Rao lower bound as described by Rye and Hardesty (1993) and require knowledge of the following parameters together with SNR:

- ratio of the lidar detector photon count to the speckle count
- receiver bandwidth
- number of pulses averaged per profile
- number of points sampled within a range gate.

The velocity uncertainty is then:

$$\sigma_e{}^2 = \left(\frac{\Delta v^2\sqrt{8}}{\alpha N_p}\right)\left(1+\frac{\alpha}{\sqrt{2\pi}}\right)^2,$$

a function of the signal spectral width, Δv, accumulated photon count, N_p, and the ratio of the lidar detector photon count to the speckle count, α. The choice of signal spectral width influences the uncertainty; Pearson et al. (2009) suggested a value of 1.5 m s^{-1}, whereas O'Connor et al. (2010) suggested a value of 2 m s^{-1}.

The ratio of the lidar detector photon count to the speckle count is determined from SNR and the ratio of the signal spectral width to the receiver bandwidth:

$$\alpha = \left(\frac{SNR}{\sqrt{2\pi}}\right)\left(\frac{B}{\Delta v}\right)$$

where B is the receiver bandwidth. The accumulated photon count is determined from

$$N_p = SNR\; n\; M,$$

where n is the number of pulses averaged per profile and M is the number of points sampled within a specified range gate to obtain a raw velocity.

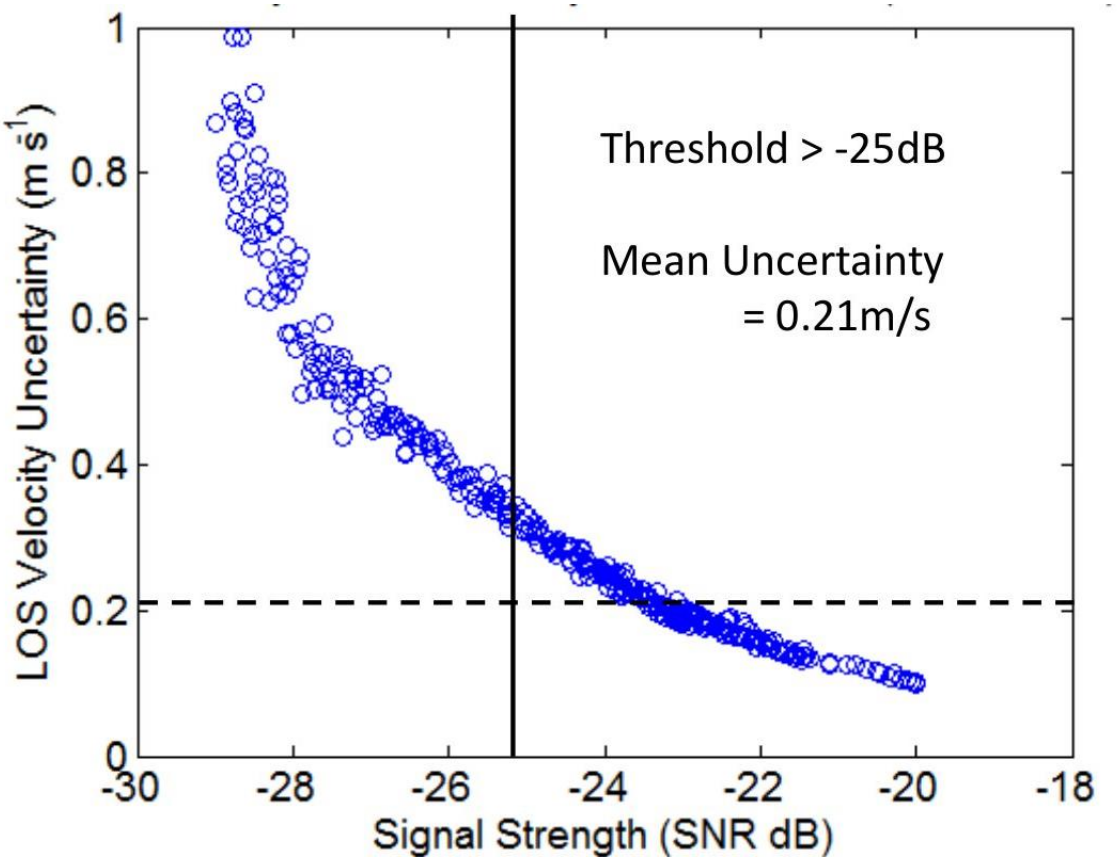

Figure 1: Velocity uncertainty versus SNR for a Leosphere Windcube 200S operating during the XPIA experiment at Boulder, US, with 50 m range resolution and 0.5 second time resolution. Courtesy of W. Brewer et al.

The signal uncertainty can then be defined as:

$$\frac{\Delta SNR}{SNR} = \frac{1}{\sqrt{n}} \frac{1}{1 + SNR}$$

Leosphere profiles have been checked to see if they match the calculated Cramer-Rao lower bound as described by Rye and Hardesty (1993), and using the operating parameters supplied by Leosphere, the theoretical calculation was a good fit to the data given in Fig. 1. In addition, extending the averaging time and range resolution had the expected improvement on the velocity and signal uncertainty in line with that predicted by theory. This allows a suitable function to be created which will derive the uncertainties for all scan types and configurations, as long as the necessary parameters are available in the files.

Note that, due to oversampling and subsequent averaging, the final range gate length does not necessarily coincide with the pulse length. In addition, Leosphere apply an

apodisation function within each range gate, which will modify the accumulated photon count slightly; **the impact of this will be checked**.

Check background

A reliable SNR/CNR is therefore required to derive uncertainties in both the velocity and the signal. SNR is derived using the background noise value, and Manninen et al. (2015) showed that it is important to examine this carefully to obtain reliable SNR estimates for the Halo Photonics lidar and post-process with a new background noise value if necessary. Here we also examine whether the Leosphere system experiences similar issues with the background.

As shown in Jana Preissler's report, the background noise value for the Leosphere system at Mace Head in Ireland is usually constant with range as required. However, there are occasions where this is not the case, as shown for the morning of 17th March 2016. To calculate CNR, the Leosphere system estimates a 'noise floor' spectra from the pre-trigger data, i.e. while the receiver is recording data before the pulse is sent out. Problems with incorrect SNR profiles were seen to arise when there was a problem with the pre-trigger data and hence the calculation of the noise spectra (see Fig. 2). The noisy peaks are seen at the low-frequency end of the spectra.

This can impact both CNR and velocity at weak SNR (< -20 dB). However, the impact is not seen at higher SNR once the 'true' observed velocity peaks dominate the 'noise' peaks in the spectra.

It is possible to identify when there is a poor estimate of the noise floor spectra and thus flag the profile. In principle, it is possible to reconstruct the entire profile from the spectra (if recorded) using a corrected noise floor spectrum.

Leosphere will look into how to determine when the pre-trigger data is reliable so that profiles can be flagged automatically and also investigate whether correcting the spectra can be automated.

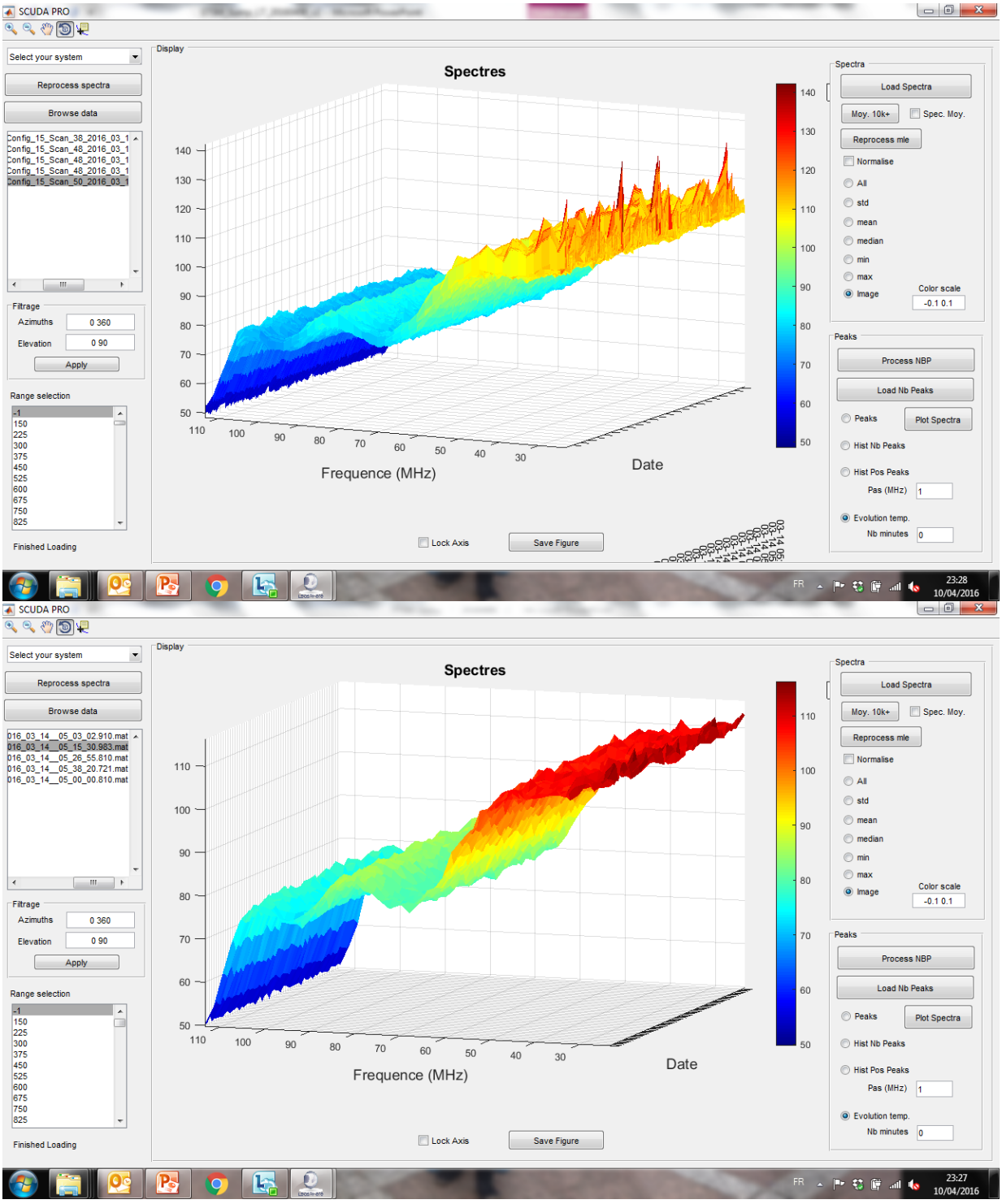

Figure 2: Bad (upper panel) and good (lower panel) noise spectra obtained using the Leosphere SCUDA tool. Note the occasional peaks at the orange/red of the colour scale.

Telescope focus – theoretical considerations

Very powerful atmospheric lidar systems (such as Raman systems) have the transmitter and receiver elements offset from one another to prevent the very strong returns from near-range over loading the detector chain.

Understanding the fraction of emitted light that is backscattered therefore requires knowledge of how the field of view of the telescope overlaps the transmitted cone of light. With full overlap, the amount of light received from a given target will reduce linearly with respect to the range squared for a telescope with the focus set at infinite.

Full overlap is often only achieved at ranges of 1 km or more from the instrument. Obtaining quantitative information below this therefore requires determination of the overlap function, which is not possible to do analytically (Sassen and Dodd, 1982) and must be obtained experimentally (Wandinger and Ansmann, 2002).

Most commercial Doppler lidar systems utilise a co-axial laser transmitter and receiver telescope, similar to many ceilometer instruments. This arrangement is possible due to the much lower laser output. Hence there is, in principle, no overlap issue, although there are often other near-range optical effects. For instance, in contrast to ceilometers, because the telescope design is diffraction-limited the signal response with range does not quite follow a range-squared law at mid to near ranges. The particular telescope setup used for Doppler lidar systems also permits the choice of modifying the telescope focus to improve the sensitivity at particular ranges. The telescope focus therefore has a large impact on the signal received at different ranges. Analogous to the overlap function, obtaining quantitative backscattering information from Doppler lidar instruments requires determination of a telescope focus function, $T_f(z)$ that varies with range z. The general lidar equation can then be written so that the attenuated backscatter profile $\beta'(z)$ is given by

$$\beta'(z) = C\, S(z) T_f(z),$$

where C is the lidar calibration constant, and $S(z)$ is the observed signal.

If the lidar laser beam and telescope specifications are known it is then possible to derive an approximate $T_f(z)$ from knowledge of the laser wavelength, laser beam diameter and telescope focal length assuming a Gaussian beam shape. Full calibration, C, also requires knowledge of additional parameters including the laser beam energy and receiver bandwidth.

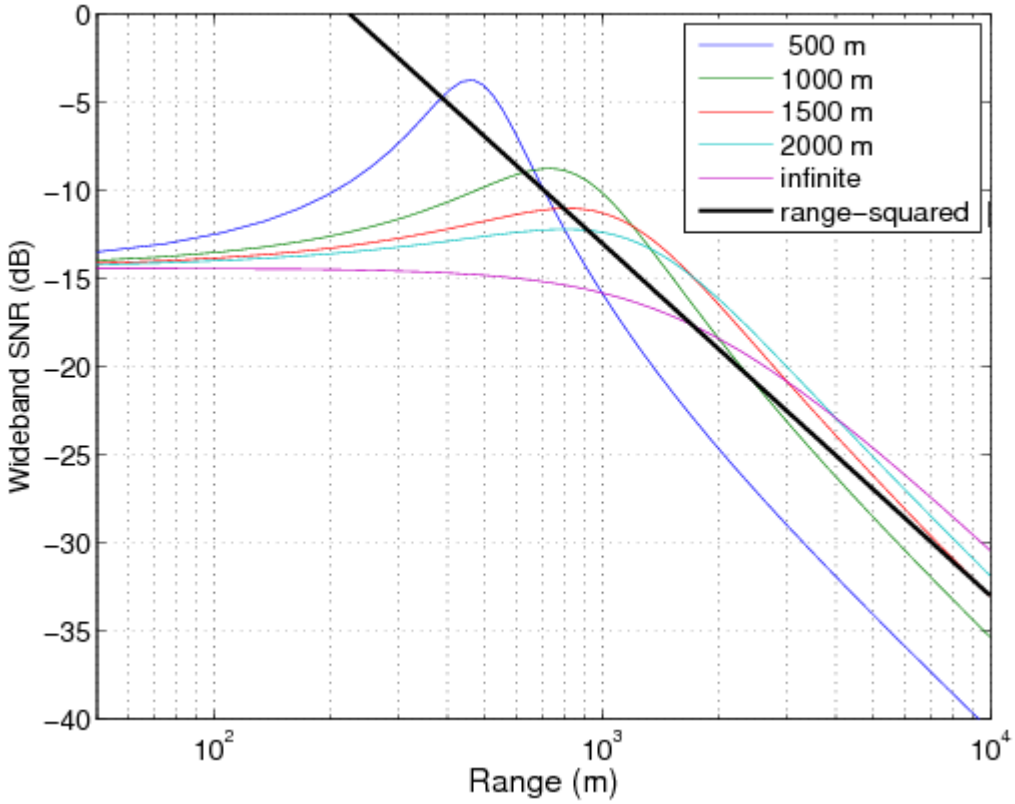

Figure 3: Impact of changing telescope focus for a constant signal, together with a reference range-squared response. Curves are for a monostatic telescope with a lens diameter of 8 cm illuminated by a Gaussian beam.

Theoretical curves for $T_f(z)$ are given in Fig. 3 for a monostatic telescope with a lens diameter of 8 cm illuminated by a Gaussian beam and show that the signal response with range does not follow a range-squared law until the far range, even with the telescope focus set to infinity.

The apparent focus is typically greater than the telescope focal length and also depends on the telescope lens diameter (Fig. 4). Note that $T_f(z)$ varies over many orders of magnitude so that any uncertainty in the instrument setup will have a major impact on the attenuated backscatter; thus it is crucial to obtain a reliable $T_f(z)$ and quantify the potential uncertainty.

The uncertainty analysis is presented in Fig. 5, where the relative change in SNR is given after the telescope focus and lens diameter are each modified by 5 and 10% from the original dimensions of: telescope focus at 1 km, lens diameter of 9 cm. As expected, a reduction in the telescope focus causes a relative increase in SNR at ranges closer than the focus, and a decrease at ranges beyond the focus; with the opposite occurring for an increase in the focal length. However, the uncertainty is not quite symmetric with respect to uncertainty in the focal length; a reduction in the focus of 10 % leads to a

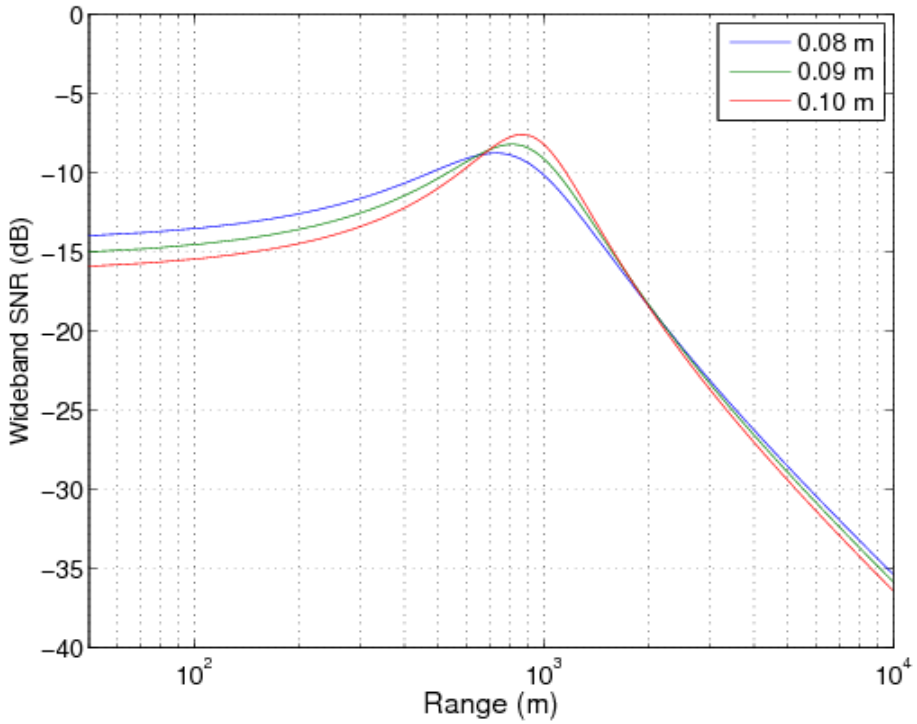

Figure 4: Impact of telescope lens diameter on distance to beam waist (apparent focus) for a constant signal and focal length. Curves are for a monostatic telescope with a focal length of 1 km illuminated by a Gaussian beam.

maximum departure of 22 % in the near range and a 10% increase in the focus leads to a departure of about 16 % in the near range. Similarly, uncertainty with respect to the telescope lens diameter is not symmetric; a reduction in the lens diameter of 10 % leads to a maximum departure of 24 % in the near range and a 10% increase in the lens diameter leads to a departure of about 17 % in the near range. Uncertainty in the lens diameter has a smaller impact at ranges beyond the focus, reaching to about 10 % for an uncertainty of 10% in the lens diameter.

Small variations in the laser output quality, which will impact how it illuminates the telescope lens on transmission, will cause fluctuations around the mean $T_f(z)$ and, if they can be assumed to be Gaussian in nature, can be expressed in terms of the relative change given in Fig. 5. For variations of less than 5 %, the uncertainty estimate can be assumed to be symmetric; larger uncertainties display a bias depending on their sign. Errors in measuring the telescope focal length and lens diameter will therefore cause gross errors in the derived attenuated backscatter profile, even if the other calibration terms (e.g. laser beam energy) are known accurately, leading to biases in both the near range (affecting aerosol) and far range (ice cloud). It is not yet known what the typical uncertainties in focus length and lens diameter are (for all systems, not just Leosphere).

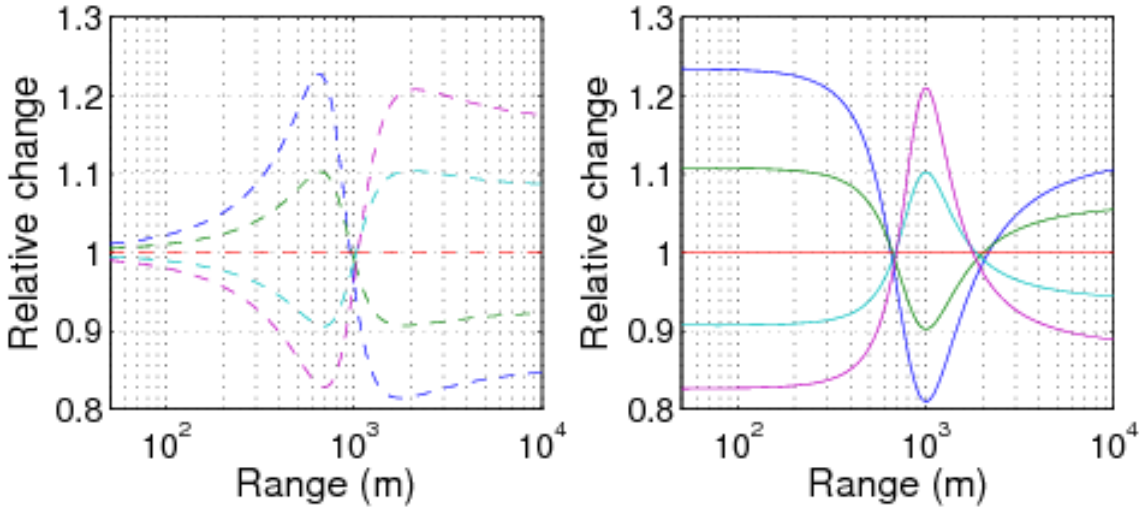

Figure 5: Uncertainty in $T_f(z)$ for a 5 and 10% change in telescope focus (left panel) and in lens diameter (right panel), relative to a monostatic telescope with a focal length of 1 km and lens diameter 9 cm illuminated by a Gaussian beam. Blue (-10 %), green (-5 %), cyan (+5 %), magenta (+10 %).

Note that the telescope function should also include some element of atmospheric dispersion, hence the difficulty in applying a pure analytical solution. The impact of atmospheric dispersion has not yet been taken account in this initial uncertainty analysis.

Telescope focus – practical considerations

If the lidar telescope parameters are already known with sufficient accuracy, then a suitable $T_f(z)$ can be chosen and modified slightly to fit the observations, as discussed in Hirsikko et al. (2014). Another method can be used when the instrument parameters are not known in advance. This makes use of observed CNR profiles in assumed homogeneous aerosol conditions, most likely achieved for PPI scans at low elevation.

The observed CNR profile in ideal conditions has a shape that can be fitted with a 4-parameter Lorentzian function:

$$F(z) = y_0 + \frac{2A}{\pi}.\frac{w}{4(z - x_0)^2 + w^2},$$

where y_0 describes the offset, A is the peak area, x_0 is the peak centre, and w is the width of the peak measured as the full width at half maximum (FWHM). The four parameters can be separated into those which correspond to the telescope parameters

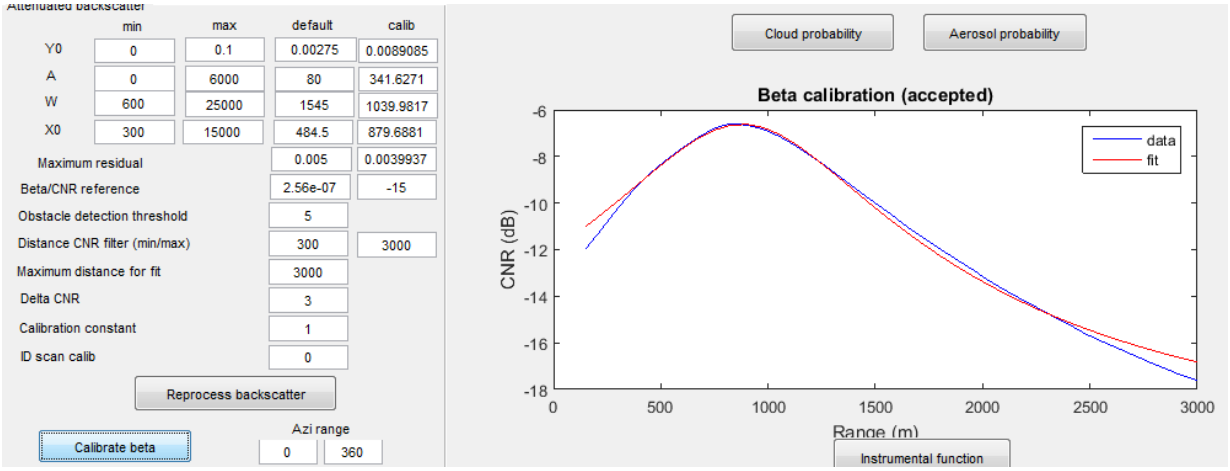

Figure 6: Leosphere SCUDA calibration tool, applied to data from a low elevation PPI scan at Mace Head, Ireland on 17th March 2016.

(x_0, w) and those which correspond to the signal strength parameters (A, y_0). The offset parameter y_0 is the noise floor. The parameter x_0 is effectively the distance to beam waist and is closely linked to the telescope focus length, bearing in mind the impact of the lens diameter on apparent focus (see Fig. 4).

Leosphere provides a calibration tool (SCUDA software) for estimating the various parameters in this function (Fig. 6), and this was applied to data from Mace Head. Applying this calibration tool to multiple scans then gives an estimate of the variability in the function parameters, as shown in Fig. 7. The telescope parameters (x_0, w) are reasonably constant throughout the day, except for the final scan, with x_0 = 880 m +/- 50 m, and w = 900 +/-150 m. An uncertainty in the focus length of 6 % will therefore lead to an uncertainty in $T_f(z)$ of about 20 % (+/- 10 %) according to Fig. 5. The parameter A varies considerably over time, as this represents the range-integral of the attenuated backscatter which changes depending on the amount of aerosol present in the atmosphere. The presence of rain or cloud (fog) in particular scans will render the atmosphere inhomogeneous with respect to CNR and the fitting tool may return a set of function parameters that are not applicable (i.e. last scan of the day in Fig. 7). Therefore, automatic calibration be used with care; it is suggested that **a manual check be applied before utilising the parameter fit given by the SCUDA tool**.

All fitting methods should also take in to account the impact of aerosol extinction, as this will reduce the SNR/CNR profile progressively with range. However, determination of the extinction profile requires an inversion method with a reliable attenuated backscatter and lidar ratio profile. Accurate determination of the extinction profile from Doppler lidar profiles alone will require an iterative procedure as the derived extinction profile will depend on the derived attenuated backscatter profile and therefore the selected telescope parameters.

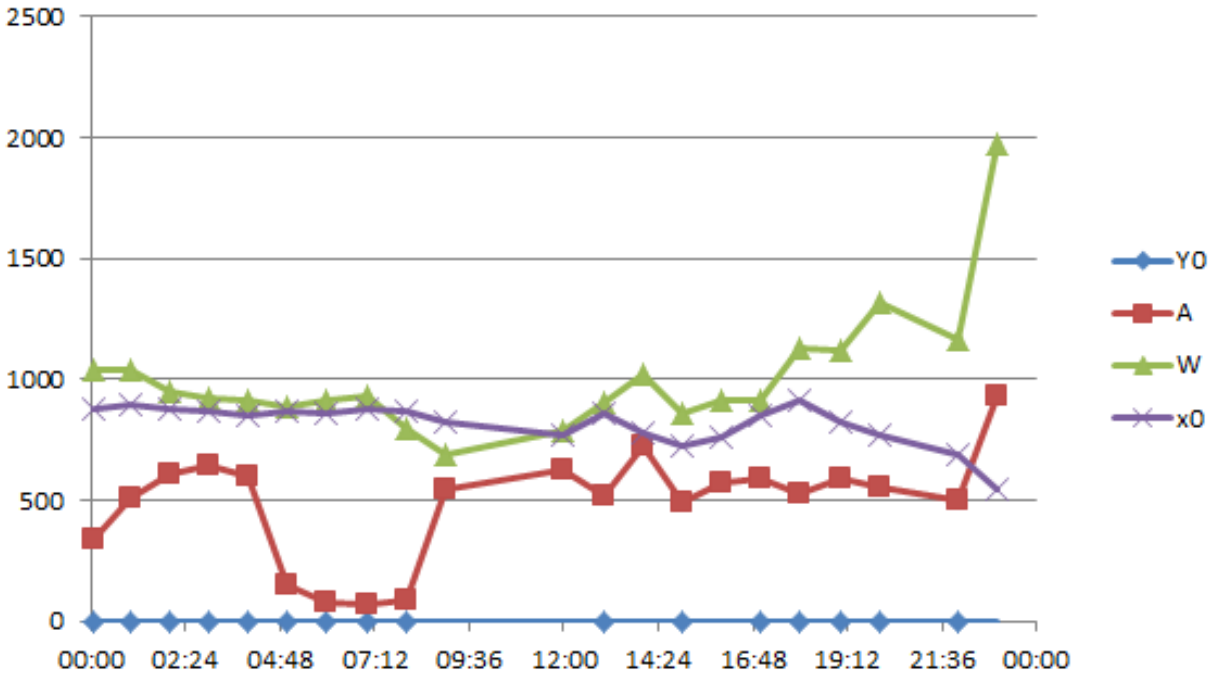

Figure 7: Results from Leosphere SCUDA calibration tool for a set of low elevation PPI scans from one day (17th March 2016) at Mace Head, Ireland. The apparent focus is represented by x0 and is reasonably constant over time.

Uncertainty in attenuated backscatter

The uncertainty in the attenuated backscatter profile $\beta'(z)$ can then be calculated from the signal uncertainty and the uncertainty in the telescope focus correction:

$$\frac{\Delta\beta'}{\beta'}(z) = \sqrt{\left(\frac{\Delta S(z)}{S(z)}\right)^2 + \left(\frac{\Delta T_f(z)}{T_f(z)}\right)^2}.$$

This provides the random error; however potential biases due to uncertainties in measuring the telescope function (shown in Fig. 5) should also be reported. Regular intercomparisons with other lidar instruments (e.g. ceilometer or Raman lidars) will be necessary to identify potential biases (Hirsikko et al., 2014). Once the telescope function can be applied, full calibration to obtain a quantitative $\beta'(z)$ is then achieved with knowledge of the transmitted energy. This can be checked through use of the lidar cloud calibration technique (O'Connor et al., 2004; Westbrook et al., 2010).

Similar to the overlap function, assuming that an analytical function can be defined for the telescope function $T_f(z)$ will not take into account the impact of imperfections in

instrument manufacture and thermal/misalignment effects; allowance for these should also be included in the uncertainty calculations.

Future plans

The harmonisation of the processing framework will continue, with the provision of common code where appropriate within the framework to ensure the creation of harmonised products from all measurement systems. This modular framework and code reuse will aid debugging, ensure common data formats and attributes are used, provide relevant uncertainties, and minimise differences in processing. The following items still require attention to check that reliable uncertainty estimates are being derived for data obtained from the Leosphere systems:

- whether chirp correction is necessary
- variability in the telescope parameters (focus length and beam/lens diameter)
- impact of the apodisation function on uncertainty estimates
- influence of unreliable noise spectra

In addition these topics will also be investigated:

- detection and correction or flagging of winds outside the Nyquist range
- detection and flagging of signals that are beyond the unambiguous range

These issues are most likely to occur when operating at low elevation angles and mitigation is possible through use of data obtained from higher elevation angles. Note that signals beyond the unambiguous range are especially likely when scanning the horizon to obtain returns for hard targets for calibration.

The scientific report will be posted on the TOPROF website: www.toprof.eu.

COST is supported by
the EU Framework Programme
Horizon 2020

References

Hirsikko, A., E. J. O'Connor, M. Komppula, K. Korhonen, A. Pfüller, E. Giannakaki, C. R. Wood, M. Bauer-Pfundstein, A. Poikonen, T. Karppinen, H. Lonka, M. Kurri, J. Heinonen, D. Moisseev, E. Asmi, V. Aaltonen, A. Nordbo, E. Rodriguez, H. Lihavainen, A. Laaksonen, K. E. J. Lehtinen, T. Laurila, T. Petäjä, M. Kulmala, and Y. Viisanen (2014): Observing aerosol particles, clouds and boundary layer wind: a new remote sensing network in Finland. *Atmos. Meas. Tech.,* **7**, 1351–1375.

Manninen, A.J., O'Connor, E.J., Vakkari, V., and Petäjä, T. (2016). A generalised background correction algorithm for a Halo Doppler lidar and its application to data from Finland. *Atmos. Meas. Tech.,* **9**, 817–827.

O'Connor, E. J., Illingworth, A. J., and Hogan, R. J. (2004): A technique for autocalibration of cloud lidar, *J. Atmos. Ocean. Tech.*, **21**, 777–786.

O'Connor, E.J., Illingworth, A.J., Brooks, I.M., Westbrook, C.D., Hogan, R.J., Davies, F., and Brooks, B.J. (2010). A Method for Estimating the Turbulent Kinetic Energy Dissipation Rate from a Vertically Pointing Doppler Lidar, and Independent Evaluation from Balloon-Borne In Situ Measurements. *J. Atmos. Ocean. Tech.*, **27**, 1652–1664.

Pearson, G., Davies, F., and Collier, C. (2009). An Analysis of the Performance of the UFAM Pulsed Doppler Lidar for Observing the Boundary Layer. *J. Atmos. Ocean. Tech*., **26**, 240–250.

Rye, B. J. and R. M. Hardesty (1993): Discrete spectral peak estimation in incoherent backscatter heterodyne lidar. I: Spectral accumulation and the Cramer-Rao lower bound. *IEEE Trans. Geosci. Remote Sens.,* **31**, 16–27.

Sassen, K., and G. C. Dodd (1982): Lidar crossover function and misalignment effects. *Appl. Opt.,* **21**, 3162-3165.

Wandinger, U., and A. Ansmann (2002): Experimental determination of the lidar overlap profile with Raman lidar. *Appl. Opt*., **41**, 511-514.

Westbrook, C. D., Illingworth, A. J., O'Connor, E. J., and Hogan, R. J. (2010): Doppler lidar measurements of oriented planar ice crystals falling from supercooled and glaciated layer clouds, *Q. J. Roy. Meteorol. Soc*., **136**, 260–276.